Design and evaluation of a fast Fourier transform-based nonlinear dielectric spectrometer

Ernesto F. Treo[1,a] and Carmelo J. Felice[1,2]
[1]*Departamento de Bioingeniería, Laboratorio de Medios e Interfases, Facultad de Ciencias Exactas y Tecnología (FACET), Universidad Nacional de Tucumán (UNT), CC327, Correo Central, CP4000 San Miguel de Tucumán. Tucumán, Argentina*
[2]*Instituto Superior de Investigaciones Biológicas (INSIBIO), Consejo Nacional de Investigaciones Científicas y Técnicas (CONICET). CC327, Correo Central, CP4000 San Miguel de Tucumán. Tucumán, Argentina*

(Received 4 June 2009; accepted 23 September 2009; published online 4 November 2009)

Nonlinear dielectric spectroscopy of micro-organism is carried out by applying a moderate electrical field to an aqueous sample through two metal electrodes. Several *ad hoc* nonlinear spectrometers were proposed in the literature. However, these designs barely compensated the nonlinear distortion derived from the electrode-electrolyte interfaces (EEI). Moreover, the contribution of the suspension is masked by the effect of the nonlinearity introduced by the electrode contacts. Conversely, the nonlinear capability of a commercial tetrapolar analyzer has not been fully investigated. In this paper a new nonlinear tetrapolar spectrometer is proposed based on a commercial linear apparatus and *ad hoc* control and signal processing software. The system was evaluated with discrete electronic phantoms and showed that it can measure nonlinear properties of aqueous suspension independently of the presence of EEI (ANOVA test, $p > 0.001$). It was also tested with real aqueous samples. The harmonics observed in the current that circulates through the sample reveals useful information about the transfer function of the sample. The total harmonic distortion was computed for linear mediums. Values lower than -60 dB suggest that the system has enough capability to perform nonlinear microbiological analysis. Design specifications, sources of interference, and equipment's limitations are discussed. © *2009 American Institute of Physics.*
[doi:10.1063/1.3247903]

I. INTRODUCTION

Nonlinear dielectric spectroscopy is a noninvasive technique proposed to monitor biochemical and metabolic aspects of biological suspensions.[1] It is based on an enzyme-related electrochemical energy conversion, and it can be characterized by the generation of harmonics in the polarization current when a micro-organism suspension is exposed to a sinusoidal electric field.

The first microbiological dielectric spectrometer was developed in the 1990s by the group of Woodward and Kell.[1–5] It consisted of a tetrapolar cell filled with a suspension of micro-organisms, with a constant sinusoidal voltage generator connected to the outer electrodes. The voltage between a pair of inner electrodes was measured and frequency analyzed with Fourier series. Harmonics of the fundamental applied frequency were observed and some biochemical and biological conclusions were raised based on this analysis. The biological sample displayed *nonlinear* properties, in the sense that it generated harmonics, at relatively modest exciting fields.[6,7]

Biological materials are, in nature, aqueous phases with high ionic content. Every time a metal is sunken or contacted to such suspension, a very unpredictable electrode-electrolyte interface (EEI) impedance is established between them.

Likewise, two nonidentical EEIs are established in tetrapolar cells. Linear impedance measurements may be corrected using the four-electrodes technique[8,9] or off-line processing.[10] However, these interfaces will also behave as a nonlinear element, whose impedance depends on voltage and frequency of the applied signal.[11,12] In Woodward's design, these nonlinear EEIs distorted the current waveform and the voltage measured in the suspension reflected such distortion (see reference spectrum, in Fig. 3 of Ref. 1). Thus, the results were affected by the very unpredictable EEIs contribution. In order to minimize interfaces interference, Woodward used a second cell filled with supernatant (linear medium) as a reference. A power spectrum was obtained from each cell and test and reference spectra (expressed in decibel) were subtracted.

According to Woodward's statement, this approach allowed them to separate the electrochemical nonlinearities from the biological ones. This approach did not prove to be effective enough. Later on, polymeric-coated electrodes and artificial networks-based analysis[13–15] were also tested to reduce the EEIs interference. Other authors even partially repeated Woodward's finding but none of them solve the EEIs

[a]Author to whom correspondence should be addressed. Present address: Gabinete de Tecnología Médica (GATEME), Departamento de Electrónica y Automática (DEA), Universidad Nacional de San Juan (UNSJ), and also Consejo Nacional de Investigaciones Científicas y Técnicas (CONICET), Av Libertador 1109 Oeste, CP5400, San Juan, Argentina. Electronic mail: etreo@gateme.unsj.edu.ar. Tel.: +54(264)4211700/ext 313.

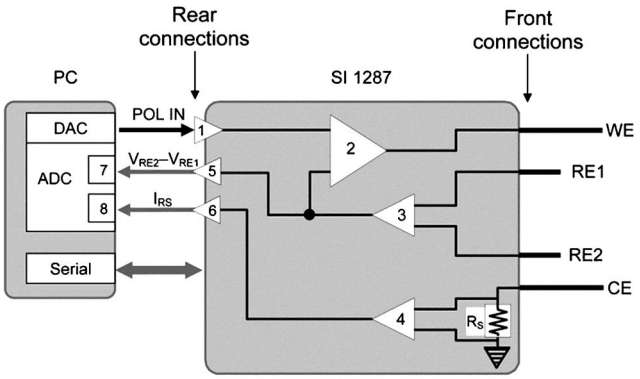

FIG. 1. Nonlinear dielectric spectrometer. (1) SI1287 input signal with ×1 or ×0.01 selectable gain, (2) gain control unit, (3) and (4) differential amplifiers used to measure voltage and current, (5) and (6) SI1287 rear output drivers used to communicate voltage and current signals with a ×1 or ×10 selectable gain, (7) and (8) ×1, ×2, ×5, and ×50 selectable gain input amplifiers included in the ADC. Serial: Serial port, I_{RS} current waveform measured on R_S.

issue.[16–22] At the moment, there are no reports about spectrometer that provides true information about the linear/nonlinear dielectric properties of aqueous suspensions.

This paper presents and evaluates a tetrapolar nonlinear spectrometer. The purpose is to overcome the EEIs difficulties mentioned above and to use the equipment in nonlinear analysis of aqueous suspensions. However it does not deal with microbiological (linear or nonlinear) analysis, and biophysical considerations will be considered in a separate paper. The system was tested with electronically simulated samples and real aqueous samples. The total harmonic distortion (THD) of the equipment was measured as an indicator of its performance. The results suggest that (i) the system can readily avoid the nonlinear EEIs disturbances, and (ii) the THD measured with linear mediums was low enough to perform nonlinear analysis of biological mediums.

II. NONLINEAR SPECTROMETER

The proposed spectrometer system is an *ad hoc* solution made to improve the performance of a commercial analyzer Solartron SI1287 (Solartron, Hampshire, England). The SI1287 unit, a very precise power source, is designed to polarize electrochemical cells or EEIs with dc or slowly variable voltages. However, it can accept externally generated voltages waveform, which enables frequency and nonlinear analysis. The entire set, depicted in Fig. 1, is composed by the electrochemical analyzer and the central personal computer (PC), which is furnished with a multifunction board (National Instruments, Texas, USA). A Windows-based application running on the PC communicates digital instructions so as to configure the SI1287 via serial port. It also manages digital-to-analog and analog-to-digital conversion between the inputs and outputs of the SI1287 and the PC, via the multifunction board. The software was implemented in MATLAB.

Briefly, the PC generates a sinusoidal waveform and then the SI1287 is used as an intermediary to apply that same voltage waveform to the sample under test (SUT). Simultaneously, the current that circulates through the SUT is measured and communicated to the PC for further digitizing and processing. The nonlinear analysis is based on the Fourier transform of the current signal.

The SI1287 has both frontal and rear connections. The former are used to attach the SUT to the unit, and the latter are used to connect the unit to the PC. Front connectors are divided into two pairs. One pair (working and counter electrode, WE and CE) is internally connected to a variable power source and used to deliver a controlled voltage, while the other pair (reference electrodes 1 and 2, RE1 and RE2) is used to sense the voltage difference between them. The name of the connectors corresponds to the standardized electrochemical terminology. Each connector is matched to one electrode of a typical longitudinally disposed tetrapolar cell;[8] the outer electrodes of the cell are connected to WE and CE, and the inner ones are connected to RE1 and RE2, respectively.

Once frequency and voltage are selected by the user to evaluate the sample, the PC uses these values to generate a digital sine wave. This digital signal (called POL IN in Fig. 1) is converted by the digital-analog converter (DAC, 16 bits, ±10 V) at a variable sampling frequency and communicated to the SI1287 rear input with shielded cables. This POL IN signal serves as reference to the gain unit of the SI1287, i.e., the unit adjusts the voltage applied between CE and WE until the voltage measured between RE1 and RE2 is equal to POL IN. The voltage waveform between RE1 and RE2 will follow the sinusoidal input signal POL IN, regardless of any load connected between RE1 and RE2 or between inner and outer electrodes.

The SI1287 is provided with a known resistance connected in series to the cell where voltage is measured. This resistance, called sensing resistance (R_S), is used to calculate current. Voltage measured on R_S along with the voltage measured between RE1 and RE2 are communicated to the PC via two analog rear outputs of the SI1287. These voltage and current outputs of the SI1287 are then digitized by the analog-to-digital converter (ADC) provided in the multifunction board (16 bits, selectable dynamic range) at a variable sampling frequency.

Four different mechanisms are used to achieve the best signal-to-noise relationship (SNR) and they take advantage of the entire dynamic range of the converters:

- Whenever the peak amplitude of the POL IN signal is smaller than 100 mV, the signal generated in the PC will be amplified ×100 and the gain of the SI1287 input driver will be switched to ×0.01.
- The R_S of the SI1287 can be switched ranging from 0.1 Ω to 10 MΩ in decades. The peak voltage in the R_S must be lower than a fixed threshold (Th). Thus, when the voltage in R_S is higher than Th, the resistance used is switched by the first lower one, and when the voltage is lower than $Th/10$ it is switched by the first higher one. The SI1287 operates upon a threshold Th value of 200 mV, the full scale range of its internal voltimeters. The same value was employed during the software design.
- The ADCs have a dynamic range selectable between ±10,

±5, ±1, and ±0.2 V and, thus, voltage resolution of 305, 152, 30.5, and 6.10 μV can be obtained.
- The output drivers of the SI1287 also have a ×1 or ×10 selectable amplifier.

All these working parameters (R_S, dynamic range of the ADC, and gain of the SI1287 outputs) are selected by the software and used to reconstruct the signal amplitude after acquisition. After both voltage and current signals were digitized, current is calculated upon the resistance used, and signals are processed as follows.

A. Signal processing

Theoretically, a sine wave concentrates all of its energy at a single frequency. To find the root-mean-square (rms) value of a harmonic, the magnitude of the FFT value is simply computed at the single frequency of that harmonic. However, the FFT of a sine wave is usually nonzero in a band of frequencies around the fundamental due to leakage from the fundamental to other frequencies.[23] In order to eliminate leakage, an integer number of cycles must be sampled. Also, for a better spectral estimate, the Welch periodogram method[24,25] was used. Consequently, sampling frequencies and acquisition length are carefully set as follows:

(i) The ADC and DAC sampling frequency were selected to be a multiple (64) of the signal frequency. This value was called sampling-signal relationship (*SSr*). However, the multifunction board can only run in predetermined sampling frequency values, as defined by its internal operating clock. Thus, the POL IN signal's frequency was slightly shifted to match exactly a ratio of 1:64 with the sampling frequency. The signal's frequency changes by less than 0.01% during this procedure. The *SSr* value is selected arbitrarily, and other values could be selected.

(ii) The periodogram method consists of dividing the signal into a finite number of shorter and possibly overlapping sections. A single frequency spectrum $h(f)$ is obtained for each section, and an average frequency spectrum $\hat{H}(f)$ is obtained with all the spectra. We chose the length of each section as $SSr \times sRes$, where *sRes*, namely, sampling resolution, stands for the amount of entire cycles contained in that section. It determines the frequency separation between fundamental frequency and its harmonics. Two consecutive sections have an overlapping of $SSr \times sRes - 1$ samples. If the number of sections is defined as av, the number of samples ns to be acquired for each signal can be calculated as $ns = SSr \times sRes + (av - 1)$, with a sampling frequency of $sf = f \times SSr$. The final spectral estimate is calculated as $20 \times \log_{10}(|\hat{H}(f)|) \times [\mathrm{dB}]$.

The amplitude corresponding to the first five harmonics is extracted from each spectrum and graphed (as function of frequency and applied voltage) into a surface plot. The signal processing and graphing stage is summarized in Fig. 2. Algebraic operations (sum, subtraction, average, and standard deviation) can be later performed upon these harmonic surfaces.

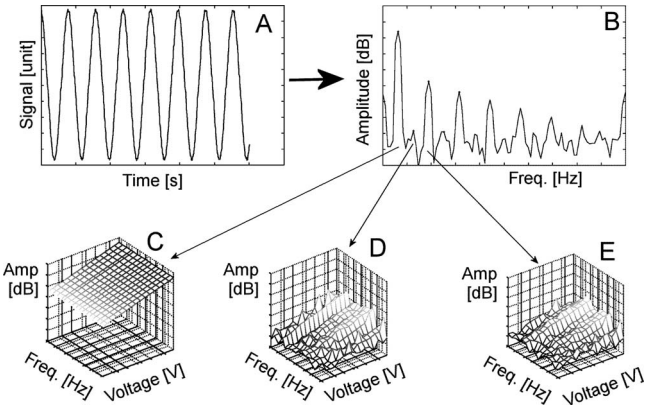

FIG. 2. Summary of the digital processing stage. The digitized signal (whether voltage or current) (a) is frequency transformed by means of the periodogram method. A frequency spectrum (b) is obtained for each signal. The amplitude measured at the fundamental frequency and its harmonics is extracted and each one is plotted in a separate tridimensional surface (subsets c–e, only the first three harmonics were schematized). The surfaces are plotted as a function of the magnitude and frequency of the applied voltage signal.

B. System evaluation

According to the SI1287 terminology, the system is operated as *potentiostat*, i.e., the voltage between the reference electrodes is controlled at a fixed level. Harmonics are expected to appear only in the current waveform. Thus, the capability of the equipment to perform linearity assessment relies in the following assumptions:

(i) The $\Delta V_{\mathrm{RE2\text{-}RE1}}$ voltage is a sine wave (with no harmonic content) independently of any nonlinear SUT or EEI connected between reference electrodes or between reference and outer electrodes, respectively.

(ii) In such case, the harmonic content observed in the current signal will only depend on the linear/nonlinear impedance of the SUT.

(iii) As corollary, a linear SUT will show none (or negligible) harmonic content in the current.

(iv) The nonlinear characteristic of the SUT should be the same regardless of any EEI connected to the system (between inner and outer electrodes).

Therefore, measurements on phantom circuits and statistical analysis were carried out to validate these hypotheses. Initially, two types of SUT phantoms (linear and nonlinear) were tested. Each phantom was tested connected to the analyzer *without any* EEI, as depicted in Fig. 3(a), up. In this arrangement, referred as *configuration #1*, the front connectors of the SI1287 were matched in pairs and both interfaces were neglected. After completing these two experiments, the front connectors of the SI1287 were rearranged into the *configuration* #2 [Fig. 3(a), down]. In this configuration, one of the EEIs was modeled with a nonlinear phantom and the other was neglected.

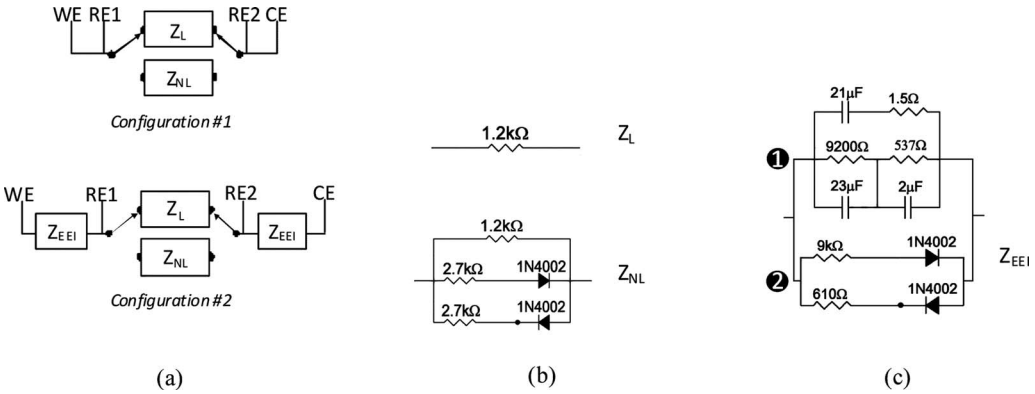

FIG. 3. Connection schemes, phantoms, and cell used to test the spectrometer. Subset (a) shows the configuration of the analyzer in the (up) absence and (down) presence of an EEI, called configurations #1 and #2, respectively. WE, CE, RE1, and RE2 correspond to the standard terminology of the front connectors of the SI1287. Subset (b) shows both (up) linear and (down) nonlinear phantoms, and (c) shows the nonlinear EEI phantom.

Consequently, four different experiments were carried out. The voltage and current waveforms digitized in each experiment were stored and off-line processed to perform the statistics described below. Voltage ($\Delta V_{\mathrm{RE2\text{-}RE1}}$) was used to test hypothesis 1, whereas current waveform analysis was used to validate the hypothesis 2–4.

The four experiments were performed, varying both frequency and voltage applied, between 1–1000 Hz (logarithmic scale, 16 points) and 50–5000 mV (logarithmic scale, 16 points). Each complete measurement was repeated 10 times. The sample size (n) for each experiment was 2560 ($n=16\times16\times10$). All voltages are rms values.

1. Linearity descriptor

Nonlinearity of passive electronic components is typically described as the deviation of the true electric response of the element from its ideal transfer function straight line. In active electronic components, linearity is rather a measure of unwanted harmonics generated by the device when a sinusoidal signal is used as an input. It is typically presented as the ratio between the root square magnitude of harmonics with respect to the fundamental amplitude. When a sine wave is used as an input to the system, the THD can be measured at any point as[25,26]

$$\mathrm{THD}_{\mathrm{dB}} = 20\ \log_{10}\left(\frac{\sqrt{S_2^2+S_3^2+S_4^2+\ \ldots\ +S_n^2}}{S_1}\right),$$

where S_1, $S_2\ldots S_n$ are the rms amplitude of the fundamental and its n harmonic, respectively, of the signal S.

2. Voltage statistics

Hypothesis 1 refers to whether the voltage can be trusted as a sine wave or not, in spite of any linear/nonlinear SUT or EEI. Consequently, THD was calculated on voltage signals by taking into account up to the fifth harmonic. The rms harmonics amplitude (V_1, $V_2\ldots V_5$) were obtained from the voltage power spectrum $\hat{H}_V(f)$. 2560 THD values were obtained for each experiment, then, they were averaged to summarize each experiment.

The harmonic content generated by an electronic nonlinear system depends, among other parameters, on the magnitude of the voltage applied. Thus, each voltage signal was analyzed in order to verify that its amplitude is as expected. The rms amplitude of each signal was computed as $x_{\mathrm{rms}}=\sqrt{x_1^2+x_2^2+\ldots+x_n^2/n}$, where x is an n-samples voltage signal. The relative voltage error for each signal was then estimated as $\mathrm{err}[\%]=100|(x_{\mathrm{rms}}-x_{\mathrm{exp}})/x_{\mathrm{exp}}|$, where x_{exp} is the expected rms voltage. These data (2560 values) were averaged so as to estimate the mean error in the rms amplitude for each experiment.

3. Current statistics

The current signal was analyzed to validate hypothesis 2, 3, and 4. Hypothesis 2 and 3 can be evaluated by means of the THD measured for the current signals, both in the linear and nonlinear SUT. The rms harmonics amplitude (I_1, $I_2\ldots I_5$) were obtained from the current power spectrum $\hat{H}_I(f)$. For each experiment 2560 THD values were obtained, which then were averaged to summarize each experiment.

Hypothesis 4, however, states that the harmonic content of any SUT must be the same whether measured in configuration #1 or #2 [as depicted in Fig. 3(a)]. The harmonic amplitudes measured with each configuration were statistically tested for that purpose. This procedure was performed for both the linear and nonlinear SUT phantom. The analysis of variance (ANOVA) is the model that best suits the statistical requirement. The purpose of ANOVA is to test differences in means (between groups or variables) for statistical significance. If significant, the null hypothesis (of no differences between means) is rejected, and the alternative hypothesis (means are different from each other) is accepted. Factorial ANOVA is used when the effects of two or more treatment variables (or factors) are being analyzed.

The statistical analysis was carried out by using voltage and frequency of the applied signal, harmonic number (1–5) and configuration (#1 or #2) as factors. Fundamental and harmonic amplitudes (first to fifth harmonic, expressed in decibel) of the current signal were used as a dependent variable. Factorial ANOVA provides a p-value for each predictor. Significant values for the type of measurement would indicate that the harmonics amplitude of the SUT is statistically different when measured in configuration #1 or #2.

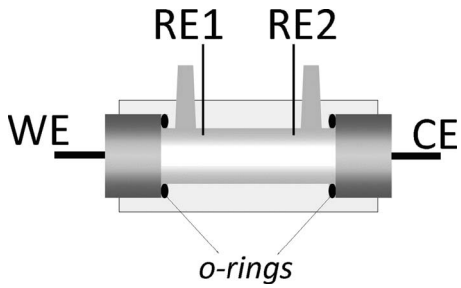

FIG. 4. Tetrapolar cell used to measure nonlinear properties of aqueous solutions.

4. Phantom design

Phantoms were designed with passive electronic components, and nonlinear behavior was approached by using standard diodes. All three phantoms shown in Figs. 3(b) and 3(c) nearly emulate the impedance of real elements.

The impedance of a suspension of *Saccharomyces cerevisiae* (as described in Ref. 1) was measured with the tetrapolar cell depicted in Fig. 4 and a Solartron 1250 frequency response analyzer (commanded by the software provided by the manufacturer, Zplot ®). The cell has two lateral flat stainless steel AISI 304 electrodes, polished with sandpaper (grit 600, Buehler, Illinois, USA) and two inner stainless steel wired electrodes (Dentaurum, Buenos Aires, Argentina). The cylindrical cell has an internal diameter of 10 mm, with the outer electrode threaded at both sides sealed with o-rings and separated 40 mm. Each inner electrode is located 5 mm from the outer electrode, respectively, and the separation between them is 30 mm. The impedance of the yeast sample was ~1.1 kΩ and so the linear phantom impedance Z_L was modeled with a 1.2 kΩ resistance (Fig. 3(b), up). Thereafter, the medium was supposed to be nonlinear and two symmetrical branches (Fig. 3(b) down) with diodes were connected in parallel to the resistance. The resistance of these branches was selected to produce harmonics similar to those ones reported by Woodward[1] (close to −35 dB as relative to the fundamental amplitude).

The phantom presented in Fig. 3(c) emulates the EEI of an AISI 304 stainless steel electrode in saline solution. The electrode was hand polished with 3 μm grinding diamond past and measurements were carried on a standard tripolar cell.[12] The phantom was devised to have a frequency and voltage dependent impedance by means of a linear frequency-dependent branch, in parallel with a nonlinear frequency-independent branch, respectively, as it has been proposed.[27]

The linear frequency response of the EEI was measured with the Solartron 1250 frequency response analyzer (1 Hz–1 kHz, 50 mV_{rms}) and fitted to the upper branch of the circuit (labeled as 1 in the figure) by using the software provided by the manufacturer (Zplot® and Zview ®).

The dc response of the EEI was measured with the Solartron 1287 unit and with the software provided by the manufacturer (in the ±0.5 V range at a scan rate of 5 mV/s, CorrWare® and CorrView®). Anodic and cathodic linear regions of the voltage-current plot were fitted to linear equations and resistance of each one was derived. The lower branch of the model, composed by these resistances in combination with diodes, is responsible for the nonlinear behavior of the EEI model. The average THD of the interface model was −36.5 dB ± 13.6 dB. The resistance tolerance was 5% in all cases.

C. Measurements with saline solution

We also measured the nonlinear response of an aqueous sample of saline solution (NaCl 0.9%) in the tetrapolar cell shown in Fig. 4. We performed measurements with this cell in real bipolar and tetrapolar configurations resembling *configurations #1* and #2, respectively. However, the EEI cannot be disregarded and, consequently, the bipolar measurement should reflect its nonlinear behavior. On the other hand, tetrapolar configuration should compensate such distortion and reveal a linear medium. The frequency and voltage ranges are 1–100 Hz, 16 logarithmic steps, and 100–1500 mV, 16 logarithmic steps.

III. RESULTS

A. Voltage analysis

The results of the THD analysis performed on voltage signal are presented in Table 1 (column 3). All four experiments revealed an averaged value close to −66 dB ± 7 dB, with maximum and minimum values close to −61 and −90 dB, respectively. None of the computed THD values were higher than −60 dB.

The error analysis carried out of the voltage signals is shown in column 5. The rms amplitude measured shown an averaged absolute error close to 0.24% for all four experiments.

B. Current analysis

Ten THD surfaces were obtained for each experiment. They were averaged to provide a single plot for each experiment, and they are shown in Fig. 5. Initially the results for the linear SUT are analyzed. There were no observable differences when the type of configuration was changed [Figs. 5(a) and 5(b)]. Both surfaces showed amplitudes slightly below −60 dB for the smallest voltage value, and they decreased as the voltage increased, as low as −75 dB. When all data were averaged, the mean THD was −63.3 dB ± 5.11 dB and −63.2 dB ± 5.21 dB for configurations #1 and #2, respectively.

The nonlinear phantom was then analyzed, and the surfaces obtained are also very similar [Figs. 5(c) and 5(d)]. Predictably, the THD was strictly dependent on the voltage applied. The value was lower than −60 dB for low voltages and, as voltage increases up to 170 mV, the distortion of the systems also increases up to a maximum of −36 dB, observed at 538 mV. The average THD was −41.7 dB ± 13.1 dB for both experiments. The standard deviation of these surfaces was much greater than those observed for the linear medium, due to the nature of the SUT.

When measured in bipolar configuration the aqueous sample showed high THD, mainly for low frequencies and high voltages [−25 dB for 1 Hz and 1500 mV, Fig. 5(e)]. As frequency increases and voltage decreases, the harmonic

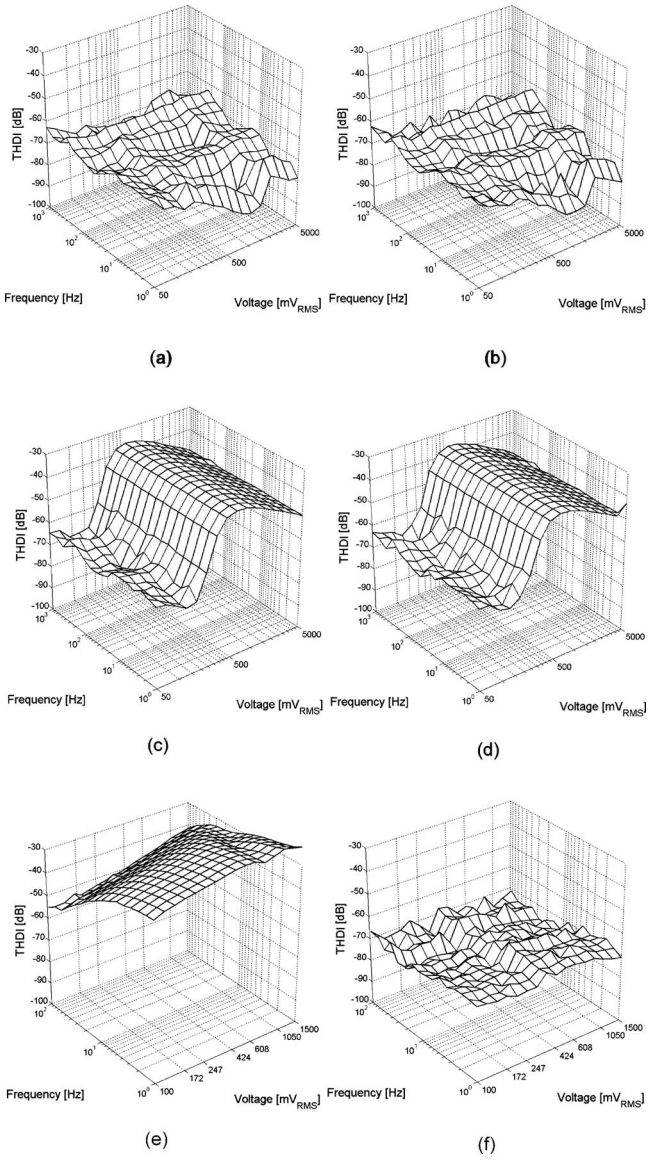

FIG. 5. Total harmonic distortion calculated for the phantoms and test cell: (a) Linear sample measured in configuration #1, (b) linear sample connected to the nonlinear interface in configuration #2, (c) nonlinear sample in configuration #1, (d) nonlinear sample connected to the nonlinear interface in configuration #2, (e) saline solution in bipolar configuration, and (f) saline solution in tetrapolar configuration.

content drops down to −60 dB. The surface was almost flat for the tetrapolar configuration [Fig. 5(f)], with values ranging from −66 to −80 dB, very similar to the linear resistance. The average standard deviation was 8.96 and 4.99 dB in the bipolar and tetrapolar configurations, respectively.

Results of the ANOVA analysis are shown in Table I. The results showed significant values ($p<0.001$) for frequency, voltage, and harmonic, and no significant values for both configurations ($p=0.609$ and $p=0.012$ for linear and nonlinear phantom, respectively). In consequence, evidence is not enough to reject the null hypothesis (no difference between means) and, finally, it is accepted. It was found that the harmonic amplitude measured in each experiment depends on voltage and frequency of the input signal, and also on the number of harmonic being analyzed. However, this amplitude does not depend on the configuration used during the experimental procedure.

IV. DISCUSSION

The tetrapolar method, developed before the 1900,[9] is the most accepted technique for reducing errors due to the electrode polarization impedance in biological measurements. Many studies have even been carried out about the performance of such systems,[28] but none have been focused on the usefulness (or not) of such devices in nonlinear analysis. In this paper the tetrapolar technique was tested with electronic phantoms and the analysis was focused on the interfaces generated at the injection electrodes. It was not analyzed nor taken into account any possible polarization effect between the potential-sensing electrodes. This polarization can be critical in higher-frequency analysis because the input impedance of the analyzer can be degraded by the parasitic capacitance at the reference electrodes (>10 GΩ and 50 pF, respectively, as reported by the manufacturer).

We exploited the capability of a linear electrochemical analyzer to perform nonlinear analysis. The voltage analysis revealed an acceptable THD (<−60 dB) in the voltage signal for all four experiments. There is also a good correlation between expected and measured rms voltage (all errors were lower than 1%). These two results well verified the first hypothesis stated in materials and methods.

When analysis was based on the current through the SUT, the harmonic content depended on its linear/nonlinear transfer function. When the SUT had a linear transfer function, the THD measured was negligible (<−60 dB). When the SUT was a nonlinear circuit, harmonics appeared only in the current waveform with a voltage-dependent behavior. Hypothesis 2 and 3 were also verified.

Finally, the statistic analysis applied to current signals suggests that tetrapolar configuration can measure the har-

TABLE I. Results of the statistical analysis. First column indicates the SUT (phantom/cell) used, and the second column indicates the type of measurement performed. THDV means total harmonic distortion measured in the voltage signal, and THDI means total harmonic distortion measured in the current signal. Er: Absolute relative error ± standard deviation. Asterisk indicates that the p-value observed is <0.001.

SUT	Configuration	THDV [dB] Mean ± sd	THDI [dB] Mean ± sd	Er [%] Mean ± sd	p values observed for predictors: Frequency	Voltage	# of harmonic	Configuration
Linear phantom	#1	−67.1 ± 7.04	−63.3 ± 5.11	0.24 ± 0.17	*	*	*	0.609
	#2	−66.8 ± 7.45	−63.2 ± 5.21	0.25 ± 0.17				
Nonlinear phantom	#1	−66.8 ± 7.28	−41.7 ± 13.1	0.24 ± 0.17	*	*	*	0.012
	#2	−66.7 ± 7.25	−41.7 ± 13.1	0.24 ± 0.17				

monic distortion produced by the SUT regardless of any nonlinear EEI connected in between. Both types of configuration provided the same harmonic information related to the SUT, whether graphically or statistically. Hypothesis 4 was also validated.

Frequency, voltage, and harmonic influence somehow the nonlinear response ($p<0.001$). However, for an entirely frequency-independent linear medium (as the resistance used here) it is expected to have a frequency-voltage independent response. This unpredicted result will be analyzed in detail. The influence of these two parameters (frequency and voltage of the input signal) was analyzed in the measured harmonic amplitude, and two distinctive sources of variations were found,

(i) when the current flowing through the internal resistance (R_S) increases, it causes the voltage measured by the internal SI1287 voltmeter to exceed a limit. Then, R_S is switched by a ten times lower one. The voltage generated is, in consequence, ten times smaller and the SNR is deteriorated also by a decade. If the medium is linear, there are no harmonics, and the surfaces reflect the noise baseline of the spectrums. If the SNR decreases, the baseline moves up and the relative amplitude between fundamental and harmonics decreases.

(ii) In spite of the careful setting of the signal and sampling frequencies, there is still an electric noise different from 50 Hz (or its harmonics), which may appear at a fixed frequency (aliased radio frequency or power source noise). Narrow peaks appear at those frequencies. Whenever any harmonic lies in one of those frequencies, the measured value is biased and the difference between fundamental and harmonics amplitude is also reduced [see frequencies higher than 100 Hz in Figs. 5(a) and 5(b)].

Voltage and frequency showed also significant ($p<0.001$) values for the nonlinear phantom (Table I). Voltage of the input signal does affect the harmonic amplitude, as observed in Figs. 5(c) and 5(d). This predictable behavior of the nonlinear circuit explains by itself the significant value obtained. However, the nonlinear phantom is independent on the frequency, and no significant values should have been observed. The power line noise observed and discussed in the linear phantom analysis was also responsible for the p value obtained for the nonlinear phantom.

The quantization process due to the digital converters (ADC and DAC) may produce harmonics of the fundamental signal.[29] A simulation was performed to measure the amplitude of such harmonics in this device. It was found that the quantization harmonics are not significant (less than -70 dB as measured to the fundamental amplitude). These amplitudes are smaller than the averaged THD computed for linear medium and thus, quantization harmonics are too small to be observed. Neither quantization harmonics nor electronics-originated harmonic were observed in the power spectrums analyzed.

A threshold of 200 mV was used to switch the sensing resistance R_S, as it was described in materials and method section. However, as this design actually does not make use of the SI1287's voltmeters, the threshold adopted could be significantly higher. This may allow a better SNR in the current signal and an improvement in the THD values. This hypothesis is being validated by our group.

The harmonic analysis on voltage signals revealed a sinusoidal signal with a THD lower than -60 dB, for both SUTs. Although commercial generators with a higher THD performance are available in the market, none of them provides tetrapolar nonlinear analysis, and this impairment has been solved by the device proposed in this paper. If a THD improvement is desired, a single compact unit which includes all the functions hereby proposed can be designed, where susceptibility to external noise is minimized. Nevertheless, the THD performance is good enough to register the nonlinear dielectric properties of biological suspensions, according to previous reports.[1–5,15,19–21]

V. CONCLUSION

It has been statistically proved that the spectrometer provides nonlinear information of the mediums, and it is able to eliminate the nonlinear interference of other systems connected in series, such as the EEIs in aqueous suspensions. A radical difference of the device proposed respect to previous design, lies in the feedback control unit which adjust the voltage measured between VR1 and VR2 in order to match the reference supplied by the DAC.

Noise rejection must be emphasized if better THD values are required. The analysis due to the combination of resistances and amplification stages here provided is not limited by the analog/digital converters resolution and it rather depends on the noise of the acquired signals. If SNR is improved, results independent from the frequency voltage and better THD performance will probably be obtained.

ACKNOWLEDGMENTS

This work was supported by grants from the Agencia Nacional de Promoción Científica y Tecnológica (Contract No. PICTO 554-6), the Consejo Nacional de Investigaciones Científicas y Técnicas (CONICET) (Contract No. PIP 6331), the Consejo de Investigaciones de la Universidad Nacional de Tucumán (CIUNT) (Contract No. E347), and Institutional funds from Instituto Superior de Investigaciones Biológicas (INSIBIO). We also thank Professor Santiago Caminos for his valuable help in the translation of this paper.

[1] A. M. Woodward and D. B. Kell, Bioelectrochem. Bioenerg. **24**, 83 (1990).
[2] A. McShea, A. M. Woodward, and D. B. Kell, Bioelectrochem. Bioenerg. **29**, 205 (1992).
[3] A. M. Woodward and D. B. Kell, Bioelectrochem. Bioenerg. **26**, 423 (1991).
[4] A. M. Woodward and D. B. Kell, FEMS Microbiol. Lett. **84**, 91 (1991).
[5] A. M. Woodward and D. B. Kell, J. Electroanal. Chem. **320**, 395 (1991).
[6] J. Victor and R. Shapley, Biophys. J. **29**, 459 (1980).
[7] H. V. Westerhoff, R. D. Astumian, and D. B. Kell, Ferroelectrics **86**, 79 (1988).
[8] H. P. Schwan and C. D. Ferris, Rev. Sci. Instrum. **39**, 481 (1968).
[9] L. A. Geddes, IEEE Eng. Med. Biol. Mag. **15**, 133 (1996).
[10] E. F. Treo, C. J. Felice, M. C. Tirado, M. E. Valentinuzzi, and D. O. Cervantes, IEEE Trans. Biomed. Eng. **52**, 124 (2005).

[11] G. A. Ruiz, C. J. Felice, and M. E. Valentinuzzi, Chaos, Solitons Fractals **25**, 649 (2005).
[12] G. Ruiz and C. J. Felice, Chaos, Solitons Fractals **31**, 327 (2007).
[13] A. M. Woodward, E. A. Davies, S. Denyer, C. Olliff, and D. B. Kell, Bioelectrochemistry **51**, 13 (2000).
[14] A. M. Woodward, R. J. Gilbert, and D. B. Kell, Bioelectrochem. Bioenerg. **48**, 389 (1999).
[15] A. M. Woodward, A. Jones, X. z. Zhang, J. Rowland, and D. B. Kell, Bioelectrochem. Bioenerg. **40**, 99 (1996).
[16] M. J. Hutchings, B. C. Blake-Coleman, and P. Silley, Biosens. Bioelectron. **9**, 91 (1994).
[17] D. Nawarathna, J. Miller, J. R. Claycomb, G. Cardenas, and D. Warmflash, Phys. Rev. Lett. **95**, 158103 (2005).
[18] B. C. Blake-Coleman, M. J. Hutchings, and P. Silley, Biosens. Bioelectron. **9**, 231 (1994).
[19] D. Nawarathna, J. R. Claycomb, G. Cardenas, J. Gardner, D. Warmflash, J. Miller, and W. R. Widger, Phys. Rev. E **73**, 051914 (2006).
[20] D. Nawarathna, J. R. Claycomb, J. Miller, and M. J. Benedik, Appl. Phys. Lett. **86**, 023902 (2005).
[21] C. J. McLellan, A. D. C. Chan, and R. A. Goubran, "Aspects of Nonlinear Dielectric Spectroscopy of Biological Cell Suspensions," *Proceedings of the 28th IEEE EMBS Annual International Conference*, New York City, Aug. 30–Sept. 3, 2006 (IEEE, Piscataway, 2006), Vol. 455.
[22] T. Inuishi, M. Muraji, and H. Tsujimoto, Mem. Fac. Eng., Osaka City Univ. **43**, 13 (2002).
[23] J. W. Gibbs, Nature (London) **59**, 606 (1899).
[24] P. Welch, IEEE Trans. Audio Electroacoust. **15**, 70 (1967).
[25] O. M. Solomon, Jr., IEEE Trans. Instrum. Meas. **43**, 194 (1994).
[26] D. Shmilovitz, IEEE Trans. Power Deliv. **20**, 526 (2005).
[27] A. Richardot and E. T. McAdams, IEEE Trans. Med. Imaging **21**, 604 (2002).
[28] S. Grimnes and Ø. G. Martinsen, J. Phys. D: Appl. Phys. **40**, 9 (2007).
[29] K. Kim, IEEE Trans. Instrum. Meas. **43**, 151 (1994).